11th World Congress on Computational Mechanics (WCCM XI)
5th European Conference on Computational Mechanics (ECCM V)
6th European Conference on Computational Fluid Dynamics (ECFD VI)
E. Oñate, J. Oliver and A. Huerta (Eds)

SHEAR DEFORMABLE HYBRID FINITE-ELEMENT FORMULATION FOR BUCKLING ANALYSIS OF THIN-WALLED MEMBERS

R. EMRE ERKMEN*, VIDA NIKI†

* Centre for Built Infrastructure Research, Faculty of Engineering and IT, University of Technology Sydney, P.O. Box 123 Broadway, NSW, Australia. Emre.Erkmen@uts.edu.au

† Centre for Built Infrastructure Research, Faculty of Engineering and IT, University of Technology Sydney, P.O. Box 123 Broadway, NSW, Australia. Vida.Niki@student.uts.edu.au

Key Words: *thin-walled, composite, hybrid finite elements, shear deformation, buckling*

Abstract. Thin-walled members that are used in many industrial and residential structures, are susceptible to buckling due to their slenderness, because of which accurate prediction of their response is required. The effect of shear deformation can gain importance in the buckling behaviour of beams especially with built-up or composite sections or the materials with relatively low shear modulus such as FRP. To include shear deformation effects, in displacement based formulations, the kinematic assumptions of Vlasov should be modified. On the other hand, in complementary energy based formulations, shear deformations can be included by using the strain energy of the shear stresses without modifying the kinematic assumptions, however the assemblage procedure is difficult for such formulations. To overcome the shortcomings of both displacement based and complementary energy based formulations, mixed-hybrid finite element formulations can be used. In this study, the hybrid finite element formulation based on Hellinger-Reissner functional is obtained by introducing the equilibrium and force boundary conditions as auxiliary conditions to the complementary energy functional.

1 INTRODUCTION

Thin-walled structural elements are used in industrial and residential structures such as bridges, ship hulls, aircrafts and aerospace buildings. Because of their slenderness, which leads to susceptibility to buckling, their response should be predicted accurately. Closed-form solution procedures for the buckling analysis of thin-walled members which date back to nineteenth century [1-4], are limited to certain boundary conditions and type of loading. Consequently, numerical methods have been developed to be able to address general cases. For the first time, displacement-based finite element formulations were developed for flexural and lateral-torsional buckling analysis of thin-walled members [5,6].

The effect of shear deformation can gain importance in the buckling behaviour of beams especially with built-up or composite sections [7,8] or alternatively, when materials with relatively low shear modulus are used such as FRP[9,10]. In displacement based formulations, the kinematic assumptions of Vlasov [1]should be modified to include the shear deformation

effects[11,12,13,14]. On the other hand, shear deformations can be included by using the strain energy of the shear stresses in a complementary-energy based formulation [2] without modifying the kinematic assumptions [15,16]. However, the inter-element force equilibrium conditions have to be satisfied a-priori [16], which complicates the assemblage procedure [3]. Mixed-hybrid finite element formulations can be used to overcome the shortcomings of both displacement- and complementary energy-based formulations.

In this study, by introducing the equilibrium and force boundary conditions as auxiliary conditions to the complementary energy functional, the Hellinger-Reissner functional is obtained. The complementary energy that is adopted here is the one introduced by Koiter [17], in which the Jaumann stress tensor is adopted. The benefit of the hybrid formulation is that the resulting matrix equations consist of only the nodal values of displacements as unknowns. Thus, the assemblage procedure is as simple as in the case of displacement-based elements. In addition, the formulation captures the effects of load position by virtue of the freedom provided in the beam axis selection. Examples are presented herein to compare the results with solutions from literature and those based on shell element models, and to show the applicability of the proposed formulation to practical problems, and to discuss the importance of shear deformation effect.

2 DEFORMATION, ROTATION AND STRESS DEFINITION

Two coordinate systems are adopted: The spatial XYZ Cartesian coordinate system which is fixed and the material xyz curvilinear coordinate system which is changing with the structure deformation. The infinitesimal parallelepiped is deformed under the successive application of stretch, rotation and rigid translation defined by the displacement fields u_s, v_s and w_s along the X, Y and Z directions respectively.

Rotation tensor R_{ij} determines the orientation of triad $\vec{e}$ with respect to the triad $\vec{e}_0$ (Fig. 1) i.e., $e_i = R_{ij}e_{0j}$. Based on the Euler-Rodrigues formula [17], the rotation tensor is expressed in terms of three independent rotation vector components ϕ_1, ϕ_2 and ϕ_3 about the X, Y and Z direction respectively as:

$$R_{ij} = \delta_{ij}\left(1 - \frac{1}{2}\phi_k\phi_k\right) + \varepsilon_{ikj}\phi_k + \frac{1}{2}\phi_i\phi_j + o(|\phi|^3) \tag{1}$$

where ε_{imj} is the permutation symbol and $o(|\phi|^3)$ is terms with higher than the second order.

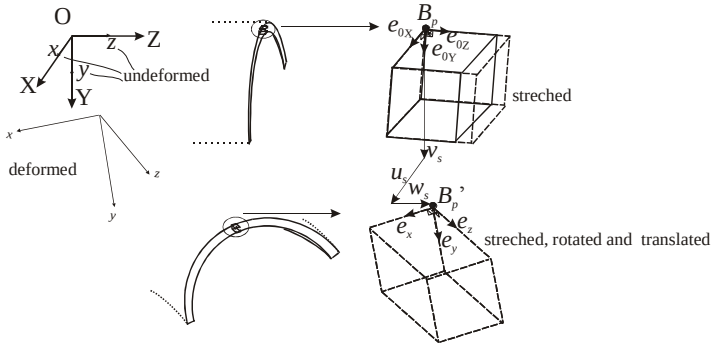

Fig.1. Deformations of an infinitesimal element of volume along principal directions observed from spatial coordinate

The forces f_X, f_y and f_z are acting on the surfaces which were initially perpendicular to X, Y and Z axes respectively. The first Piola-Kirchoff stresses D_{ij} are defined as the forces acting along X, Y and Z axes per unit of initial un-deformed area i.e., $D_{jk} = [\frac{f_j}{dx_p dx_q}] i_{0k}$, ($j \neq p \neq q$). The components i_{0X}, i_{0y} and i_{0Z} of triad $\vec{i}_0$ are unit vectors along X, Y and Z directions respectively. For isotropic materials, the Jaumann stresses σ_{ik} can be expressed in terms of the first Piola-Kirchoff stress tensor D_{ij} and the rigid body rotation tensor R_{jk} as $\sigma_{ik} = D_{ij} R_{jk}$ [17].

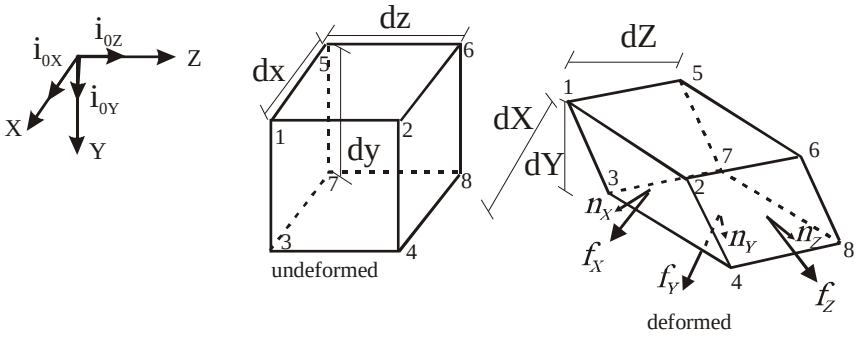

Fig. 2 Forces acting on the deformed shape observed from spatial coordinates XYZ

3 VLASOV BEAM THEORY

Based on the first Vlasov assumption, the cross-section remains rigid under deformation. Therefore, the in-plane displacements $u_s(s,z)$ and $v_s(s,z)$ of a point B_p located on the section mid-surface can be expressed in terms of the in-plane displacement components u(z) and v(z) of an arbitrarily located pole $A_p(a_x, a_y)$ and the angle of twist of the cross-section $\phi_s(z)$ (Fig. 3a). Thus

$$u_s(s,z) = u(z) - \left[y(s) - a_y \right] \sin \phi_Z(z) \approx u(z) - \left[y(s) - a_y \right] \phi_Z(z)$$
$$v_s(s,z) = v(z) + \left[x(s) - a_x \right] \sin \phi_Z(z) \approx v(z) + \left[x(s) - a_x \right] \phi_Z(z) \tag{2}$$

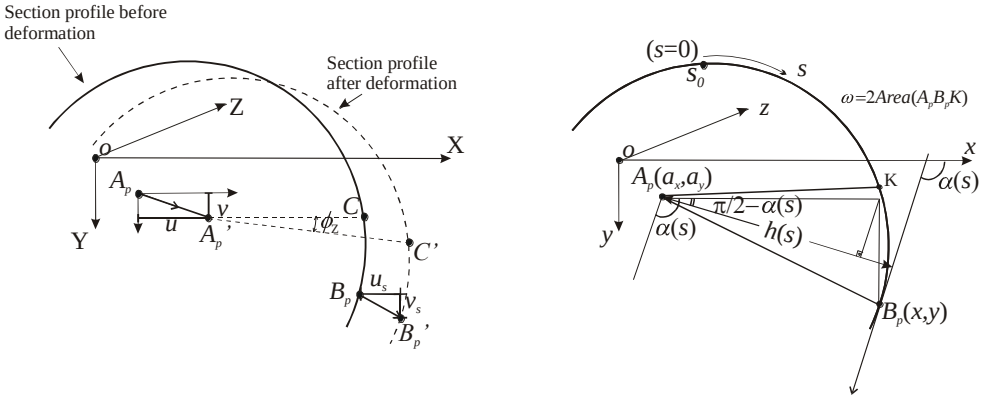

(a) Cross-section Displacements in spatial coordinates(b) Sectorial Area definition in material coordinates

Fig. 3 Displacements and coordinates of a thin-walled section

By neglecting the terms higher than second order in Eqs. (2) and taking the derivatives with respect to the longitudinal coordinate z, one obtains

$$\begin{aligned}\phi_X(z,x) &= -v'(z) - (x-a_x)\phi_Z' \\ \phi_Y(z,y) &= u'(z) - (y-a_y)\phi_Z'\end{aligned} \tag{3}$$

In line with the Vlasov theory, the stress components σ_{xx}, σ_{yy}, σ_{xy}, D_{XX}, D_{YX}, D_{XY}, D_{YY} are neglected throughout the analysis and the stress resultant functions are defined as

$$\text{(a) } N(z)=\int_A \sigma_{zz}(z,s)dA, \quad \text{(b) } M_x(z)=\int_A \sigma_{zz}(z,s)y(s)dA, \quad \text{(c) } V_y(z)=\int_A \sigma_{zy}(z,s,r)dA, \tag{4}$$

$$\text{(d) } M_y(z)=-\int_A \sigma_{zz}(z,s)x(s)dA, \quad \text{(e) } B(z)=\int_A \sigma_{zz}(z,s)\omega(s)dA, \quad \text{(f) } V_x(z)=\int_A \sigma_{zx}(z,s,r)dA,$$

$$\text{(g) } T(z)=\int_A \left\{-\sigma_{zx}(z,s,r)\left[y(s)-r\cos\alpha-a_y\right]+\sigma_{zy}(z,s,r)\left[x(s)+r\sin\alpha-a_x\right]\right\}dA$$

$$\text{(h) } T_w(z)=\int_A \left\{-\sigma_{zx}(z,s,r)\left[y(s)-a_y\right]+\sigma_{zy}(z,s,r)\left[x(s)-a_x\right]\right\}dA$$

In Eqs. (4), $\omega(s)=\int_{s_0}^{s} h(\xi)d\xi$ and $h(s)=(x-a_x)\sin\alpha(s)-(y-a_y)\cos\alpha(s)$ (Fig. 3b), coordinate r is the normal distance from the mid-surface, $dA=drds$ is an element of cross-section area in the material coordinates. The stress expressions in terms of stress resultants functions in a non-orthogonal coordinate system are adopted from [19].

$$\sigma_{zz}=\begin{pmatrix}1 & -x(s) & -y(s) & -\omega(s)\end{pmatrix}\mathbf{D}^{-1}\begin{Bmatrix}N\\ M_y\\ -M_x\\ -B\end{Bmatrix} \tag{5}$$

in which matrix $\mathbf{D}$ is given by

$$\mathbf{D}=\begin{bmatrix}A & -S_y & -S_x & -S_\omega\\ -S_y & J_{yy} & J_{xy} & J_{\omega x}\\ -S_x & J_{xy} & J_{xx} & J_{\omega y}\\ -S_\omega & J_{\omega x} & J_{\omega y} & J_{\omega\omega}\end{bmatrix} \tag{6}$$

and the section constants $A=\int_A dA$, $S_y=\int_A xdA$, $S_x=\int_A ydA$, $S_\omega=\int_A \omega dA$, $J_{xx}=\int_A y^2dA$, $J_{xy}=\int_A xydA$, $J_{yy}=\int_A x^2dA$, $J_{\omega x}=\int_A \omega xdA$, $J_{\omega y}=\int_A \omega ydA$, $J_{\omega\omega}=\int_A \omega^2dA$ are defined.

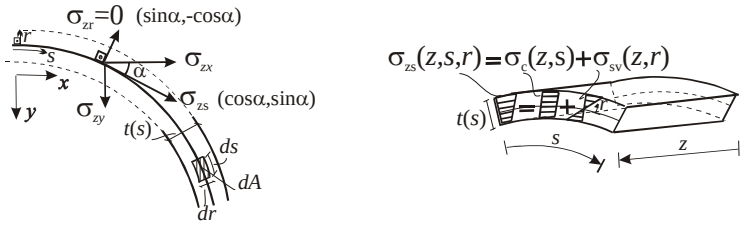

(a)Stress components on the section contour line (b) Linear and constant stress components

Fig. 4 Components of the Jaumann stresses for small deformations in line with the Vlasov theory

In line with the Vlasov theory, the Jaumann stress components σ_{zx} and σ_{zy} are expressed in terms of a stress component σ_{zs} acting in the direction tangent to the section contour line for small deformations. Also, $\sigma_{zr} = \sigma_{zx}\sin\alpha - \sigma_{zy}\cos\alpha \simeq 0$ (Fig. 4a). The stress component σ_{zs} consists of one constant component across the thickness (due to the combination of warping torsion and biaxial shear forces) and one component with a linear variation along thickness due to the St. Venant torsion (Fig. 4b). The constant stress component can be expressed in terms of the stress resultant functions as [19]

$$\sigma_c(z,s) = \frac{1}{t(s)}\left\langle \bar{A}(s) \quad -\bar{S}_y(s) \quad -\bar{S}_x(s) \quad -\bar{S}_\omega(s)\right\rangle \mathbf{D}^{-1}\begin{Bmatrix} 0 \\ V_x \\ V_y \\ T_w \end{Bmatrix} \tag{7}$$

$\vec{A}(s) = \int_{s_b}^{s} dA$, $\overrightarrow{S_y}(s) = \int_{s_b}^{s} xdA$, $\overrightarrow{S_x}(s) = \int_{s_b}^{s} ydA$ and $\overrightarrow{S_x}(s_0,s) = \int_{s_b}^{s} \omega(s_0,s)dA$ are defined, in which s_b is the coordinate s of the one of the edges of the cross-section at which Jaumann stress component $\sigma_c = (z,s)$ vanishes. The linear stress component is

$$\sigma_{sv}(z,r) = \frac{2r}{J_d}T_{sv}(z) \tag{8}$$

3.1 Notation for pre-buckling and buckling stress, rotation and displacement fields

Under a reference pre-buckling load a thin-walled alters from the undeformed state to a deformed state and will undergo a rotation tensor R_{ij}^{p} and will be subjected to the Piola-Kirchoff stress fields D_{ij}^{p} or the Jauman Stress tensor σ_{ij}^{p}. The reference load is increased by a scalar multiplier λ till the structure reaches the state of onset of buckling ($\lambda R_{ij}^{p}, \lambda D_{ij}^{p}, \lambda\sigma_{ij}^{p}$). In transforming from this point to the final buckled configuration ($R_{ij}^{*}, D_{ij}^{*}, \sigma_{ij}^{*}$), there is an increase in rotation tensor, first Piola-Kirchoff stress, and Jauman stress by ΔR_{ij}, ΔD_{ij} , $\Delta\sigma_{ij}$ respectively. The above three sets of rotation and stress fields are related through $R_{ij}^{*} = \lambda R_{ij}^{p} + \Delta R_{ij}$, $D_{ij}^{*} = \lambda D_{ij}^{p} + \Delta D_{ij}$, and $\sigma_{ij}^{*} = \lambda\sigma_{ij}^{p} + \Delta\sigma_{ij}$.

By using the relations in Eq. (4) for pre-buckled and buckled configurations and the relations $\Delta v = \Delta M_x = \Delta V_y = \Delta N = 0$ [20] and $V_x^p = M_y^p = T_w^p = T_{sv}^p = B^p = 0$ [21], one obtains

$$\sigma_{zz}^{p} = \left\langle 1 \quad -x(s) \quad -y(s) \quad -\omega(s)\right\rangle \mathbf{D}^{-1}\begin{Bmatrix} N^p \\ 0 \\ -M_x^p \\ 0 \end{Bmatrix} \tag{9}$$

$$\Delta\sigma_{zz} = \left\langle 1 \quad -x(s) \quad -y(s) \quad -\omega(s)\right\rangle \mathbf{D}^{-1}\begin{Bmatrix} 0 \\ \Delta M_y \\ 0 \\ -\Delta B \end{Bmatrix} \tag{10}$$

$$\Delta\sigma_c(z,s) = -\frac{1}{t(s)}\left\langle \bar{A}(s) \quad \bar{S}_y(s) \quad \bar{S}_x(s) \quad \bar{S}_\omega(s) \right\rangle \mathbf{D}^{-1} \begin{Bmatrix} 0 \\ \Delta V_x \\ 0 \\ \Delta T_w \end{Bmatrix} \tag{11}$$

$$\Delta\sigma_{sv}(z,r) = \frac{2r\Delta T_{sv}(z)}{J_d} \tag{12}$$

4 VARIATIONAL FORMULATION

The complementary energy expression for semilinear material under finite deformations is provided by Koiter [17] as

$$\pi_c(R_{ij}^*, \sigma_{ij}^*) = \int_{V_0} \left[\frac{1}{4G}\left(\sigma_{ij}^* \sigma_{ij}^* - \frac{\nu}{1+\nu}\sigma_{ii}^{*2} \right) + \sigma_{ii}^* - R_{ij}^* \sigma_{ji}^* \right] dV \tag{13}$$

In Eq. (13), G is the shear modulus, ν is the Poisson's ratio and V_0 is the volume of the undeformed body. Linearized buckling analysis is performed in two steps. Firstly, linear static analysis is performed under applied loads. Secondly, by using the internal forces obtained from the linear static analysis and substituting it into the stability condition, an eigenvalue problem is obtained. One can express the stability criterion based on the complementary energy as provided by Koiter [17] and Oran [18] i.e., $\delta\left(\frac{1}{2}\delta^2\pi^*\right) = 0$. For the pre-buckling analysis, i.e. $R_{ij}^* = \delta_{ij}$ and $\sigma_{ij}^* = \sigma_{ij}^p$ the complementary energy can be written as

$$\pi_c = \int_L \left\{ \frac{1}{2E}\left\langle N \quad M_x \right\rangle \mathbf{D}_p^{-1} \begin{Bmatrix} N \\ M_x \end{Bmatrix} + \frac{1}{2G} V_y^{\,2} \boldsymbol{\chi}_p^{-1} \right\} dz \tag{14}$$

in which the vanishing stress fields of the pre-buckling analysis are omitted and Eq. (9) was used. In Eq. (14), $\mathbf{D}_p^{-1}$ and $\boldsymbol{\chi}_p^{-1}$ can be written as

$$\mathbf{D}_p^{-1} = \begin{bmatrix} 1 & 0 & 0 & 0 \\ 0 & 0 & -1 & 0 \end{bmatrix} \mathbf{D}^{-1} \begin{bmatrix} 1 & 0 \\ 0 & 0 \\ 0 & -1 \\ 0 & 0 \end{bmatrix} \tag{15}$$

$$\boldsymbol{\chi}_p^{-1} = \left\langle 0 \quad 0 \quad -1 \quad 0 \right\rangle \mathbf{D}^{-1} \int_A \frac{1}{t^2} \begin{bmatrix} \bar{A}^2 & -\bar{A}\bar{S}_y & -\bar{A}\bar{S}_x & -\bar{A}\bar{S}_\omega \\ -\bar{A}\bar{S}_y & \bar{S}_y^{\,2} & \bar{S}_y\bar{S}_x & \bar{S}_y\bar{S}_\omega \\ -\bar{A}\bar{S}_x & \bar{S}_y\bar{S}_x & \bar{S}_x^{\,2} & \bar{S}_x\bar{S}_\omega \\ -\bar{A}\bar{S}_\omega & \bar{S}_y\bar{S}_\omega & \bar{S}_x\bar{S}_\omega & \bar{S}_\omega^{\,2} \end{bmatrix} dA \mathbf{D}^{-1} \begin{Bmatrix} 0 \\ 0 \\ -1 \\ 0 \end{Bmatrix} \tag{16}$$

By imposing the element equilibrium and force boundary conditions as auxiliary constraints Hellinger-Reissner functional for pre-buckling can be obtained from Eq. 14) as

$$\pi_{HR} = \int_L \left\{ M_x v'' + q_y v + N w' + q_z w - \frac{1}{2E} \begin{Bmatrix} N & M_x \end{Bmatrix} \mathbf{D}_p^{-1} \begin{Bmatrix} N \\ M_x \end{Bmatrix} - \frac{1}{2G} V_y^{\,2} \boldsymbol{\chi}_p^{-1} \right\} dz \tag{17}$$

By expanding the complementary energy functional in the neighbourhood of the buckling configuration using Taylor series, neglecting the terms higher than the second order and considering the fact that the first variation vanishes $\delta\pi_c = 0$, one obtains the second variation of complementary energy expression as

$$\begin{aligned} \delta^2\pi_c = \lambda \int_L \Big[& \Delta u'^2 N^p + 2\Delta u' \Delta\phi_Z' \left(-M_x^p + a_y N^p \right) + \Delta\phi_Z'^2 \left(r_{N0}^{\,2} + a_y^{\,2} + a_x^{\,2} \right) N^p + \Delta\phi_Z'^2 \beta_{Nx} M_x^p \Big] dz \\ + \int_L \Bigg\{ & \frac{1}{E} \begin{Bmatrix} \Delta M_y & \Delta B \end{Bmatrix} \mathbf{D}_b^{-1} \begin{Bmatrix} \Delta M_y \\ \Delta B \end{Bmatrix} + \frac{1}{G} \begin{Bmatrix} \Delta V_x & \Delta T_w \end{Bmatrix} \boldsymbol{\chi}_b^{-1} \begin{Bmatrix} \Delta V_x \\ \Delta T_w \end{Bmatrix} + \frac{\Delta T_{sv}^{\,2}}{G J_d} \Bigg\} dz \end{aligned} \tag{18}$$

in which the vanishing stress fields of the pre-buckling analysis are omitted and Eqs. (10) to (12) was used. Definitions of r_{N0} and β_{Nx} used in Eq. (18) can be found in [21]. Hellinger-Reissner functional can be obtained from the complementary energy functional by imposing the element equilibrium and force boundary conditions as auxiliary constraints [21] as

$$\begin{aligned} \frac{1}{2}\delta^2\pi_{HR} = & \frac{1}{2}\lambda \int_L \Big[\Delta u'^2 N^p + 2\Delta u' \Delta\phi_Z' \left(-M_x^p + a_y N^p \right) + \Delta\phi_Z'^2 \left(r_{N0}^{\,2} + a_y^{\,2} + a_x^{\,2} \right) N^p + \Delta\phi_Z'^2 \beta_{Nx} M_x^p \Big] dz \\ & - \frac{1}{2} \int_L \left\{ \frac{1}{E} \begin{Bmatrix} \Delta M_y & \Delta B \end{Bmatrix} \mathbf{D}_b^{-1} \begin{Bmatrix} \Delta M_y \\ \Delta B \end{Bmatrix} + \frac{1}{G} \begin{Bmatrix} \Delta M_y' & \Delta B' \end{Bmatrix} \boldsymbol{\chi}_b^{-1} \begin{Bmatrix} \Delta M_y' \\ \Delta B' \end{Bmatrix} + \frac{\Delta T_{sv}^{\,2}}{G J_d} \right\} dz \\ & + \int_L \Delta u'' \Delta M_y \mathrm{d}z + \int_L \left\{ \Delta\phi_Z'' \Delta B - \Delta T_{sv} \Delta\phi' \right\} \mathrm{d}z \end{aligned} \tag{19}$$

in which

$$\mathbf{D}_b^{-1} = \begin{bmatrix} 0 & 1 & 0 & 0 \\ 0 & 0 & 0 & -1 \end{bmatrix} \mathbf{D}^{-1} \begin{bmatrix} 0 & 0 \\ 1 & 0 \\ 0 & 0 \\ 0 & -1 \end{bmatrix} \tag{20}$$

$$\boldsymbol{\chi}_b^{-1} = \begin{bmatrix} 0 & 1 & 0 & 0 \\ 0 & 0 & 0 & 1 \end{bmatrix} \mathbf{D}^{-1} \int_A \frac{1}{t^2} \begin{bmatrix} \bar{A}^2 & -\bar{A}\bar{S}_y & -\bar{A}\bar{S}_x & -\bar{A}\bar{S}_\omega \\ -\bar{A}\bar{S}_y & \bar{S}_y^{\,2} & \bar{S}_y\bar{S}_x & \bar{S}_y\bar{S}_\omega \\ -\bar{A}\bar{S}_x & \bar{S}_y\bar{S}_x & \bar{S}_x^{\,2} & \bar{S}_x\bar{S}_\omega \\ -\bar{A}\bar{S}_\omega & \bar{S}_y\bar{S}_\omega & \bar{S}_x\bar{S}_\omega & \bar{S}_\omega^{\,2} \end{bmatrix} dA \mathbf{D}^{-1} \begin{bmatrix} 0 & 0 \\ 1 & 0 \\ 0 & 0 \\ 0 & 1 \end{bmatrix} \tag{21}$$

5 FINITE ELEMENT FORMULATION

The pre-buckling stress resultant fields for an element *i* of span *L* can be written as

$$N_i^p(z) = N_i^p \tag{22}$$

$$M_{xi}^{p}(z) = \mathbf{L}(z)^{\mathrm{T}}\mathbf{M}_{xi}^{p} \tag{23}$$

$$V_{yi}^{p} = \mathbf{L}'(z)^{\mathrm{T}}\mathbf{M}_{xi}^{p} \tag{24}$$

In which, $\boldsymbol{L}^{T}(z) = \langle (1 - z/L) \;\; z/L \rangle$ and $M_{xi}^{pT}(z) = \langle M_{xi}^{p}(0) \; M_{xi}^{p}(L) \rangle$. The finite element is obtained by using cubic interpolation for the vertical displacement $v_i^p(z)$ and linear interpolation for the axial displacement $w_i^p(z)$. Substituting above equations into Eq. (15) and taking partial derivation with respect to N_i^p, $\boldsymbol{M}_{xi}^{p}$, w_i and v_i, the Hellinger-Reissner functional for pre buckling analysis can be written as

$$\pi_{HR} = \sum_{i=1}^{N} \int_{L} \left(\left\langle \mathbf{w}_i^{p\mathbf{T}} \quad \mathbf{v}_i^{p\mathbf{T}} \right\rangle \mathbf{G}_p{}^{\mathrm{T}} \mathbf{H}_p \mathbf{G}_p \begin{Bmatrix} \mathbf{w}_i^p \\ \hline \mathbf{v}_i^p \end{Bmatrix} \right) \mathrm{d}z + \sum_{i=1}^{N} \int_{L} \left\langle \mathbf{w}_i^{p\mathbf{T}} \quad \mathbf{v}_i^{p\mathbf{T}} \right\rangle \left[\begin{array}{c|c} \mathbf{L}^{\mathbf{T}} & \mathbf{0} \\ \hline \mathbf{0} & \mathbf{N}^{\mathbf{T}} \end{array} \right] \begin{Bmatrix} q_z \\ \hline q_y \end{Bmatrix} \mathrm{d}z \tag{25}$$

where

$$\mathbf{H}_p = \left\{ \int_{L} \frac{1}{E} \left[\begin{array}{c|c} 1 & 0 \\ \hline \mathbf{0} & \mathbf{L} \end{array} \right] \mathbf{D}_p{}^{-1} \left[\begin{array}{c|c} 1 & \mathbf{0} \\ \hline 0 & \mathbf{L}^{\mathbf{T}} \end{array} \right] + \frac{1}{G} \begin{Bmatrix} 0 \\ \hline \mathbf{L}' \end{Bmatrix} \boldsymbol{\chi}_p^{-1} \left\langle 0 \;\vdots\; \mathbf{L}'^{\mathbf{T}} \right\rangle \mathrm{d}z \right\}^{-1} \tag{26}$$

$$\mathbf{G}_p = \left[\begin{array}{c|c} \int_{L} \mathbf{L}'^{\mathbf{T}} \mathrm{d}z & 0 \\ \hline 0 & \int_{L} \mathbf{L}\mathbf{N}''^{\mathbf{T}} \mathrm{d}z \end{array} \right] \tag{27}$$

And the discretized equilibrium equations of the system can be obtained as

$$\sum_{i=1}^{N} \mathbf{K}_{pi} \begin{Bmatrix} \mathbf{w}_i^p \\ \hline \mathbf{v}_i^p \end{Bmatrix} = \mathbf{F} \tag{28}$$

In which $\mathbf{K}_{pi} = \int \mathbf{G}_p^{\mathrm{T}} \mathbf{H}_p \mathbf{G}_p dz$ is the element stiffness matrix for pre-buckling analysis and $\mathbf{F}$ is the energy equivalent nodal load vector.

The buckling stress resultant fields for an element *i* of span *L* can be written as

$$\Delta M_y(z) = \mathbf{L}(z)^{\mathrm{T}} \boldsymbol{\Delta}\mathbf{M}_{yi} \tag{29}$$

$$\Delta B(z) = \mathbf{L}(z)^{\mathrm{T}} \boldsymbol{\Delta}\mathbf{B}_i \tag{30}$$

$$\Delta T_{svi}(z) = \Delta T_{svi} \tag{31}$$

in which, $\Delta\mathbf{M}_{yi}^{T} = \langle \Delta M_{yi}(0) \; \Delta M_{yi}(L) \rangle$ and $\Delta\mathbf{B}_i^{T} = \langle \Delta B_i(0) \; \Delta B_i(L) \rangle$. The finite element formulation is obtained by interpolating the lateral displacement $\Delta u_i(\mathrm{z})$ and angle of twist $\Delta\phi_i(\mathrm{z})$ using cubic polynomials.

By substituting above equations into Eq. (23) and partial derivation with respect to $\Delta\mathbf{M}_{yi}$, $\Delta\mathbf{B}_i$, ΔT_{svi}, $\Delta\boldsymbol{u}_i$ and $\Delta\boldsymbol{\varphi}_i$ the Hellinger-Reissner functional for buckling analysis is written as

$$\delta^2\pi_{HR}=\sum_{i=1}^{N}\int_L\left(\left\langle\Delta\mathbf{u}_i^{\mathbf{T}}\quad\Delta\boldsymbol{\varphi}_i^{\mathbf{T}}\right\rangle\mathbf{G}_b{}^{\mathrm{T}}\mathbf{H}_b\mathbf{G}_b\begin{Bmatrix}\Delta\mathbf{u}_i\\ \Delta\boldsymbol{\varphi}_i\end{Bmatrix}\right)\mathrm{d}z \tag{32}$$
$$+\lambda\sum_{i=1}^{N}\int_L\left\langle\Delta\mathbf{u}_i^{\mathbf{T}}\quad\Delta\boldsymbol{\varphi}_i^{\mathbf{T}}\right\rangle\left[\begin{array}{c|c}N^p\mathbf{N}'\mathbf{N}'^{\mathbf{T}} & \left(-M_x^p+a_yN^p\right)\mathbf{N}'\mathbf{N}'^{\mathbf{T}}\\ \hline \left(-M_x^p+a_yN^p\right)\mathbf{N}'\mathbf{N}'^{\mathbf{T}} & \left[\left(r_{N0}{}^2+a_y{}^2+a_x{}^2\right)N^p+\beta_{Nx}M_x^p\right]\mathbf{N}'\mathbf{N}'^{\mathbf{T}}\end{array}\right]\begin{Bmatrix}\Delta\mathbf{u}_i\\ \Delta\boldsymbol{\varphi}_i\end{Bmatrix}\mathrm{d}z$$

$$\mathbf{H}_b=\left\{\int_L\frac{1}{E}\left[\begin{array}{cc|c}\mathbf{L}&\mathbf{0}&\mathbf{0}\\ \mathbf{0}&\mathbf{L}&\mathbf{0}\\ \hline 0&0&1\end{array}\right]\left[\begin{array}{c|c}\mathbf{D}_b^{-1}&\mathbf{0}\\ \hline \mathbf{0}&\dfrac{E}{GJ_d}\end{array}\right]\left[\begin{array}{cc|c}\mathbf{L}^{\mathbf{T}}&\mathbf{0}&\mathbf{0}\\ \mathbf{0}&\mathbf{L}^{\mathbf{T}}&\mathbf{0}\\ \hline 0&0&1\end{array}\right]+\frac{1}{G}\left[\begin{array}{cc}\mathbf{L}'&\mathbf{0}\\ \mathbf{0}&\mathbf{L}'\\ \hline 0&0\end{array}\right]\boldsymbol{\chi}_b^{-1}\left[\begin{array}{cc|c}\mathbf{L}'^{\mathbf{T}}&\mathbf{0}&0\\ \mathbf{0}&\mathbf{L}'^{\mathbf{T}}&0\end{array}\right]\mathrm{d}z\right\}^{-1} \tag{33}$$

$$\mathbf{G}_b=\left[\begin{array}{c|c}\displaystyle\int_L\mathbf{L}\mathbf{N}''^{\mathbf{T}}\mathrm{d}z & 0\\ \hline 0 & \displaystyle\int_L\mathbf{L}\mathbf{N}''^{\mathbf{T}}\mathrm{d}z\\ \hline 0 & \displaystyle\int_L\mathbf{N}'^{\mathbf{T}}\mathrm{d}z\end{array}\right] \tag{34}$$

The discretized equilibrium equations of the system can be obtained as

$$\sum_{i=1}^{N}\left[\mathbf{K}_{bi}-\lambda\mathbf{K}_{gi}\right]\begin{Bmatrix}\Delta\mathbf{u}_i\\ \Delta\boldsymbol{\varphi}_i\end{Bmatrix}=0 \tag{35}$$

in which $\mathbf{K}_{bi}$ is the element stiffness matrix for buckling analysis and $\mathbf{K}_{gi}$ is the element geometric stiffness matrix.

6 APPLIACTIONS

In order to indicate the validity of the proposed solution and to discuss the importance of shear deformation effects, two examples are presented in this section. The results are compared with the results based on shell finite element analysis solutions and other closed form or numerical solutions in literature.

Two elements are developed in this study. In element BEH (Buckling Element based on Hybrid formulation), the effect of shear deformation is omitted (i.e., $\chi^{-1}\approx 0$), whereas in element BEHS (Buckling Element based on Hybrid formulation including Shear deformation), the effect of shear deformation is retained. For both examples sixteen beam elements (BEH or BEHS, as applicable) are used to model the structures. A displacement based element (called Trahair element herein), which does not include the effect of shear deformation, is also used. For buckling analysis, it has two nodes with four degrees of freedom at each node including lateral displacement, out of plane rotation, angle of twist and warping degrees of freedom. The element is implemented for finite element analysis in [22]. In the models, pinned supports means $\Delta u=\Delta\phi=0$ and $\Delta u'\neq 0, \Delta\phi'\neq 0$ and fixed supports means $\Delta u=\Delta u'=\Delta\phi=\Delta\phi'=0$. In addition, shell element models developed in ABAQUS commercial software using S4R shell elements are used for comparison purposes.

6.1 Lateral-torsional buckling of beams with double symmetric cross-section

All beams are simply supported and span 8,000 mm. The material is steel and the beam is subjected to several linear bending moment distributions. The closed form solution for the buckling moment of simply supported beam under uniform bending moment is $M_u = (\pi/L)\sqrt{EJ_{yy}GJ_d + (\pi E/L)^2 J_{yy}J_{ww}}$ (286 kNm for the case of uniform moment). For other moment gradient configurations, various codes (e.g., LRFD 1999) provide predictions of the critical moment in the form $M_{cr} = C_b M_u$ in which C_b is a constant depending on the moment gradient. Sixteen Trahair's elements are used in all cases.

Table 1: Buckling moments for simply supported beams under linear moment gradient

	(1)	(2)	(3)	(4)	(5)	(6)
	Boundary condition and Loading	ABAQUS (kNm)	LRDF (kNm)	Trahair (kNm)	BEH (kNm)	BEHS (kNm)
1	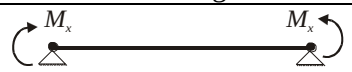	272	286 (%105)	286 (%105)	285 (%105)	285 (%105)
2	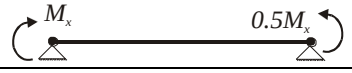	359	357 (%99.4)	376 (%105)	373 (%104)	373 (%104)
3		489	477 (%97.5)	513 (%105)	495 (%101)	494 (%101)

From Table 1, one can verify that all results are in very good agreement with the results based on ABAQUS, whose predictions are the most conservative among all while Trahair element tends to overestimate the buckling moment by 5% compared to ABAQUS results. Element BEHS provides the closest predictions to ABAQUS solution. As expected, for the 8,000 mm span members, shear deformation effects are insignificant.

6.2 Shear deformation effect in a propped cantilever with an overhang

This example is a propped cantilever with a cross section shown in Table 2 which was initially analysed by Erkmen and Mohareb [16] and used herein to illustrate the effects of shear deformation. The material properties are initially E=200GPa and G=77GPa, thus E/G ratio is 2.6. The difference between the BEH and BEHS solutions is around 10% due to the effect of shear deformation. We acknowledge that especially when the beam is short, local buckling may interact with overall buckling and influence the behaviour of the beam. In order to capture these effects, shell element models or generalized beam theory e.g., [23] can be used. In [16], by using an ABAQUS shell element model, the first mode of buckling was verified to be an overall lateral-torsional buckling mode and thus, despite a short span the beam local buckling modes did not dominate the design.

Table 2: Buckling load predictions for a propped cantilever with an overhang

Boundary Conditions and Loading	Cross-section	ABAQUS (kN)	BEH (kN)	BEHS (kN)
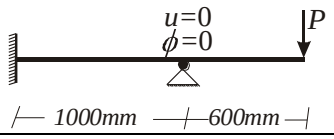	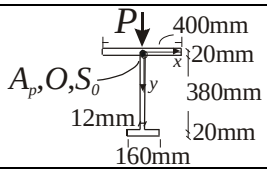	7,180	9,343 (%130)	8,499 (%118)

On the other hand, when the E/G ratio is increased to 26 by reducing the shear modulus ten times, which is a typical value for FRP pultruded [23,24] beams, the buckling load predictions based on the BEHS reduce from 8499kN to 4551kN (a reduction of some 47%). It should be noted that when the shear deformation effects are excluded, BEH predicts the buckling load as 8135kN which is 44% higher than 4551kN and thus a significant overestimation occurs for a beam consisting of a material with low shear modulus.

7 CONCLUSIONS

The finite element solution proposed in this study captures shear deformation effects in buckling analysis of thin-walled members, a feature that is neglected in most available buckling solutions. It was shown that neglecting shear deformation effects can overestimate the predicted buckling load in some cases, especially when the E/G ratio is relatively high which is the case in practice for FRP pultruded beams. Non-colinear elements can be easily connected using the developed finite element formulation as only inter-element displacement continuity is required for the assemblage procedure.

REFERENCES

[1] Michell AGM, Elastic stability of long beams under transverse forces. *Philos Mag* (1899) 48:298–309.

[2] Prandtl L. Kipperscheinungen, Doctoral dissertation, Universitat Munchen, (1899).

[3] Reissner H, Uber die Stabilitat der Biegung. *Sitzungsber Berl Math Ges Beil Arch Math Phys* (1904) III:53–6.

[4] Wagner H, Torsion and buckling of open sections. Translated technical memorandum no. 807, NACA—National Advisory Committee for Aeronautics, (1936).

[5] Krajcinovic, D., A consistent discrete elements technique for thin wall assemblages. *Int. Jour. Solids and Structures*, Vol. 5, pp. (1969) 639-662.

[6] Barsoum RJ, Gallagher RH, Finite element analysis of torsional and torsional–flexural stability problems. *Int J Numer Methods Eng* (1970) 2:335–52.

[7] T. Kant, H.S. Patil, Buckling Load of Sandwich Columns with a Higher-Order Theory. *Journal of Reinforced Plastics and Composites* (1991) 10(1): 102-109.

[8] H. Huang, G.A. Kardomateas, Buckling and initial postbuckling behavior of sandwich beams including transverse shear. *AIAA Journal* (2002) 40(11): 2331-2335.

[9] L.C. Bank, Flexural and Shear Moduli of Full-section Fiber Reinforced Plastic (FRP) Pultruded Beams. *Journal of Testing and Evaluation* (1989) 17(1): 40-45.

[10] N. Silvestre, D. Camotim, GBT buckling analysis of pultruded FRP lipped channel members. *Computers & Structures* (2003) 81: 1889-1904.
[11] V.Z. Vlasov, *Thin-walled elastic beams*, Second Edition, Israel Program for Scientific Translations, Jerusalem, Israel, (1961).
[12] M.Y. Kim, N. Kim, HT. Yun, Exact dynamic and static stiffness matrices of shear deformable thin-walled beam-columns. *Journal of Sound and Vibrations* (2003) 267: 29-55.
[13] K. Saade, B. Espion, G. Warzee, Non-uniform torsional behaviour and stability of thin-walled elastic beams with arbitrary cross-sections. *Thin-Walled Structures* (2004) 42: 857-881.
[14] Erkmen RE, Attard MM, Lateral-torsional buckling analysis of thin-walled beams including shear and pre-buckling deformation effects. *International Journal of Mechanical Sciences* (2011) 53: 918-925
[15] R.E. Erkmen, M. Mohareb, Buckling analysis of thin-walled open members-A complementary energy variational principle. *Thin-walled Structures* (2008) 46: 602-617.
[16] R.E. Erkmen, M. Mohareb, Buckling analysis of thin-walled open members-A finite element formulation. *Thin-walled Structures* (2008) 46: 618-636.
[17] Koiter, W. T., Complementary Energy, neutral equilibrium and buckling, *Proc. Kon. Ned. Akad., Wetensch., Series B*, pp.183-200 (1976).
[18] Oran, C., Complementary Energy Method for Buckling, *Journal of the Engineering Mechanics Division*, Vol. 93, No. EM1, pp. 57-75 (1967).
[19] Erkmen, R. E. and Mohareb, M. Non-orthogonal solution for thin-walled members-Generalized Expression for Stresses, *Proceedings of the Eighth International Conference on Computational Structures Technology September* (2006)
[20] Trahair, N.S., Flexural-Torsional Buckling of Structures, *CRC Press, Boca Raton, FL, USA* (1993).
[21] R.E. Erkmen, Shear deformable hybrid finite-element formulation for buckling analysis of thin-walled membres, *Finite Elements in Analysis and Design* Vol. 82 pp.32-45 (2014).
[22] Kutlukaya, O. *Lateral Stability of Planar Frames*, M. Eng. Report, University of Ottawa, ON, Canada (2003).
[23] Silvestre N, Camotim D. GBT buckling analysis of pultruded FRP lipped channel members. *Computers & Structures* (2003) 81:1889–904.
[24] Correia JR, Branco FA, Silva NMF, Camotim D, Silvestre N. First-order, buckling andpost-buckling behaviour of GFRP pultruded beams: part 1. Experimental study. In:Topping BHV, Costa Neves LF, Barros RC, editors. *Proceedings of the twelfth international conference on civil, structuraland environmental engineering computing. Stirlingshire UK: Civil-Comp Press* (2009).